2-22-2011

Tuning Lattice Thermal Conductance by Porosity Control in Ultrascaled Si and Ge Nanowires

Abhijeet Paul
NCN, Purdue University

Gerhard Klimeck
NCN, Purdue University, gekco@purdue.edu

Paul, Abhijeet and Klimeck, Gerhard, "Tuning Lattice Thermal Conductance by Porosity Control in Ultrascaled Si and Ge Nanowires" (2011). *Birck and NCN Publications.* Paper 726.
http://dx.doi.org/10.1063/1.3556648

Tuning lattice thermal conductance by porosity control in ultrascaled Si and Ge nanowires

Abhijeet Paul[a] and Gerhard Klimeck
School of Electrical and Computer Engineering, Network for Computational Nanotechnology, Purdue University, West Lafayette, Indiana 47907, USA

(Received 7 December 2010; accepted 28 January 2011; published online 22 February 2011)

Porous nanowires (NWs) with tunable thermal conductance are examined as a candidate for thermoelectric devices with high efficiency. Thermal conductance (σ_l) of porous NWs is calculated using the phonon dispersion obtained from a modified valence force field model. Porosity in the NWs break the crystal symmetry leading to the reduction in ballistic σ_l. [100] Si and Ge NWs show similar percentage reductions in σ_l for the same amount of porosity. The model predicts an anisotropic reduction in σ_l in SiNWs, with [111] showing the maximum reduction followed by [100] and [110] for a similar hole radius. The reduction in σ_l is attributed to phonon localization and anisotropic mode reduction. © *2011 American Institute of Physics*. [doi:10.1063/1.3556648]

Extreme geometrical confinement and surfaces make nanowires (NWs) a promising candidate to obtain higher efficiency (ZT) thermoelectric (TE) material by suppressing the lattice thermal conductivity (κ_l). Recent experimental works[1,2] reveal that the NW geometry can greatly enhance the ZT of Si [upto 1 at 200 K (Ref. 2)] from its bulk value of 0.06 at 300 K.[3] An interesting way to further reduce the thermal conductivity in bulk Si was shown both experimentally[4,5] and theoretically[6] by creating pores in the crystalline material. More recently the fabrication of a phonon "nanomesh"[5] showed a 100-fold reduction in κ_l from the bulk Si value of 148 to 1.9 W/m K. Recent technological developments enable the fabrication of hollow NW arrays using sacrificial templates,[7] hollow spinel wires using the "Kirkendall effect,"[8] electrochemical anodic dissolution[9] and template based hollow wire fabrication.[10] Theoretical investigation can now guide these improved fabrication methods to obtain better TE materials and structures.

Surface scattering affects phonons and the associated thermal conductivity (κ_l) more drastically than electrons, due to the smaller coherent phonon wavelength than electrons.[6] Motivated by experimental works and theoretical arguments, we analyze the ballistic thermal conductance (σ_l) in hollow Si and Ge NWs with various channel orientations ([100], [110], and [111]) to explore the candidates which lead to higher reduction in σ_l and to understand the reasons for such reduction.

The phonon dispersion in free-standing Si and Ge NWs is calculated using a frozen phonon approach, called the modified valence force (MVFF) model[11–13] [Fig. 1(a)]. In the MVFF method the frequencies of selected phonon modes are calculated from the forces acting on atoms produced by finite displacements of the atoms in a crystal at equilibrium. The MVFF model has explained the bulk phonon dispersions as well as other lattice properties in bulk Si, Ge, etc.,[11,12] and has recently been applied to SiNWs to explain their phonon spectra and lattice thermal properties.[13]

From the calculated phonon dispersion, the ballistic thermal conductance (σ_l) across a semiconductor slab/wire can be calculated using the Landauer's formula[14] using Eq. (1),[15,16]

$$\sigma_l(T) = \frac{e^2}{\hbar}\int_0^{E_{\max}} M(E)E\frac{\partial}{\partial T}\left\{\frac{1}{\left[\exp\left(\frac{E}{k_BT}\right)-1\right]}\right\}, \qquad (1)$$

where $M(E)$, k_B, $\hbar$, and e is the number of modes at energy E, the Boltzmann's constant, the Planck's constant, and the electronic charge, respectively. This equation is valid when the two contacts across the material slab are maintained under a small temperature gradient ΔT.[16]

Device details: Rectangular NWs are studied with width (W) and height (H) varying from 3 to 4 nm with three channel orientations of [100], [110], and [111]. The hole radius

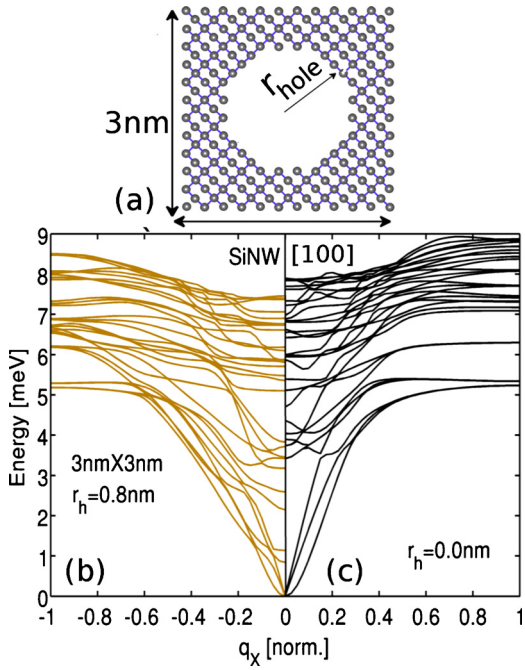

FIG. 1. (Color online) (a) Projected hollow Si unitcell with ⟨100⟩ channel orientation. Phonon dispersion obtained from the MVFF model for ⟨100⟩ (b) hollow and (c) filled SiNW with cross-section size of 3 nm(W) ×3 nm(H).

[a]Electronic mail: abhijeet.rama@gmail.com.

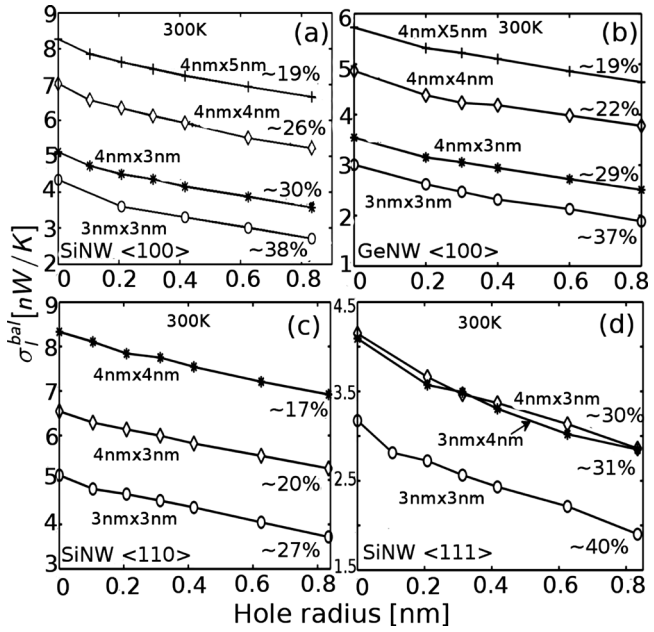

FIG. 2. Ballistic σ_l in small cross-section rectangular NWs. (a) [100] SiNW, (b) [100] GeNW, (c) [110] SiNW, and (d) [111] SiNW. The percentage reduction in σ_l for all the wires for r_h=0.8 nm is also indicated.

(r_h) in these NWs have been chosen such that not more than 25% of the total atoms [Fig. 1(a)] have been removed from the unitcell to ensure structural stability of these wires (no negative phonon dispersion is obtained[17]). The inner and outer surface atoms in these NWs are allowed to vibrate freely [Fig. 1(a)]. Extremely small SiNWs ($W \leq 1$ nm) have been excluded from the present study since significant atomic reconstruction can take place in such wires.[18]

Phonon spectra: Hollow NWs have fewer atoms per unitcell compared to the solid NWs which results in a reduced number of phonon subbands. Figures 1(b) and 1(c) compare the phonon spectra of a 3×3 nm^2 [100] SiNW with r_h=0.8 nm and 0 nm, respectively. In the hollow NW a lot of sub-branches appear in the lower energy portion of the phonon spectra [Fig. 1(b)] indicating more surface phonon confinement due to an increased surface-to-volume ratio.

Ballistic thermal conductance σ_l: In all the NWs σ_l is calculated using Eq. (1). As a general trend, σ_l reduces in hollow NWs compared to the solid NWs (Fig. 2). Comparison of σ_l in Si and Ge NW show a similar amount of reduction in thermal conductance [Figs. 2(a) and 2(b)]. This indicates a weak material dependence of the reduction mechanisms. A 3×3 nm^2 Si(Ge) NW shows a reduction of ~37%(38%) for r_h=0.8 nm. This reduction decreases as the wire cross-section size increases due to the reducing surface-to-volume ratio. The phonons feel the surface less in larger cross-section NWs compared to the smaller wires.

The σ_l reduction is wire orientation dependent as revealed in Figs. 2(a), 2(c), and 2(d). For a 3×3 nm^2 SiNW with r_h=0.8 nm, a [100] wire shows a reduction of ~38% [Fig. 2(a)], a [110] wire shows a reduction of ~27% [Fig. 2(c)] and a [111] wire shows a reduction of ~40% [Fig. 2(d)]. The σ_l reduction shows the following order [111] $\approx$[100]>[110] for all the wire cross-section sizes considered here. Thus, σ_l can be tuned by three ways, (i) wire cross-section size, (ii) hole radius, and (iii) channel orientation.

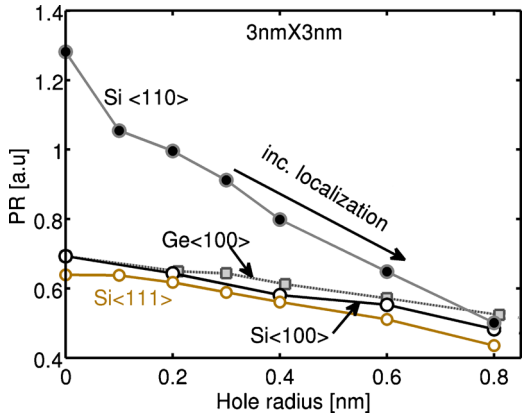

FIG. 3. (Color online) Average PR in Si and Ge NWs. PR reduces with increasing hole radius indicating increasing phonon localization in hollow NWs.

Reasons for the reduction in σ_l: The observed trends in the reduction in σ_l can be attributed to two reasons, (i) increased phonon localization in hollow NWs and (ii) anisotropic modes and mode reduction in NWs.

(a) Phonon localization: As the NW size reduces the geometrical confinement increases which results in increased phonon confinement.[19] All the phonon modes in hollow NWs do not propagate well and become localized which reduces σ_l compared to the solid Si and Ge NWs.[19,20] The extent of localization of phonon modes can be calculated using a "participation ratio" (PR).[20] The PR measures the fraction of atoms participating in a mode. This ratio can be calculated for each phonon mode as,[20]

$$\mathrm{PR}^{-1} = N\sum_i \left(\sum_{n,j\in[x,y,z]} \psi^*_{i,n,j}\psi_{i,n,j} \right)^2, \tag{2}$$

where N is the total number of atoms in the unitcell, n and j represent the number of subbands and directional vectors, respectively, and $\psi_{i,n,j}$ is the eigenvector associated with atom "i," subband "n" and direction "j." The eigenvectors are calculated from the MVFF dynamical matrix formulation as described in Ref. 12. The PR value varies between $O(1)$ for delocalized states to $O(1/N)$ for localized states and effectively indicates the fraction of atoms participating in a given mode.

The average PR in 3×3 nm^2, [100] Si and Ge NW shows a reduction with increasing r_h (Fig. 3). The solid NWs have PR close to 0.7, showing delocalization, which gradually decreases indicating phonon localization. Thus, both Si and Ge show similar phonon localization and hence similar σ_l reduction [Figs. 2(a) and 2(b)]. We therefore, predict a weak material dependence.

(b) Anisotropic phonon modes: The reduction in σ_l with channel orientation shows anisotropy due to different propagating modes [$M(E)$] for each orientation. Figure 4(a) shows that [110] wires have the largest number of modes while [100] and [111] wires have fewer modes.[15] [100] and [111] wires show similar decrease in total $M(E)$ with r_h [Fig. 4(a)] which explains the similar reduction in σ_l. The energy resolved $M(E)$ for 3×3 nm^2 SiNWs with r_h=0.4 nm [Fig. 4(b)] clearly shows higher number of modes in [110] orientation thus resulting in smaller reduction in σ_l. Phonon localization also reflects that a [111] SiNW shows similar localization as [100] SiNW whereas, [110] SiNW shows less

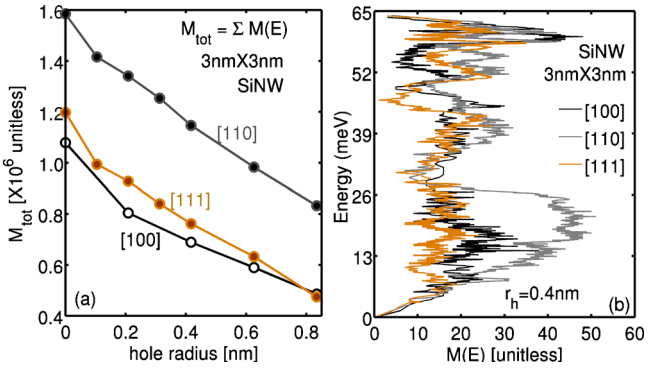

FIG. 4. (Color online) (a) Total modes in hollow SiNWs for three channel orientations with hole radius. [110] has maximum modes. [111] and [100] are very close. (b) Modes distribution in energy for three channel orientations. Both plots are for 3×3 nm^2 SiNWs.

localization (Fig. 3). This further corroborates the anisotropic reduction in σ_l in SiNWs.

It has been shown that the presence of holes in Si and Ge NWs can be used for tuning their thermal conductance. Increased phonon confinement, phonon localization due to increased surface-to-volume ratio and mode reduction are the reasons for such drastic reduction in σ_l. Thus, variation in NW cross-section size, hole radius, and channel orientation provide attractive ways to tune the thermal conductance. [100] and [111] NWs show maximum reduction in σ_l for Si. Similar trends are also expected in GeNWs. This can pave the way to make better TE devices using these NWs.

The authors acknowledge financial support from MSD Focus Center, one of six research centers funded under the Focus Center Research Program (FCRP), a Semiconductor Research Corporation (SRC) entity, Nanoelectronics Research Initiative (NRI) through the Midwest Institute for Nanoelectronics Discovery (MIND), NSF (Grant No. OCI-0749140) and Purdue University. Computational support from nanoHUB.org, an NCN operated and NSF (Grant No. EEC-0228390) funded project is also gratefully acknowledged.

[1]A. I. Hochbaum, R. Chen, R. D. Delgado, W. Liang, E. C. Garnett, M. Najarian, A. Majumdar, and P. Yang, Nature (London) **451**, 163 (2008).
[2]A. Boukai, Y. Bunimovich, J. Kheli, J. Yu, W. Goddard, and J. Heath, Nature (London) **451**, 168 (2008).
[3]T. T. Vo, A. J. Williamson, V. Lordi, and G. Galli, Nano Lett. **8**, 1111 (2008).
[4]G. Gesele, J. Linsmeier, V. Drach, J. Fricke, and R. Arens-Fischer, J. Phys. D: Appl. Phys. **30**, 2911 (1997).
[5]J.-K. Yu, S. Mitrovic, D. Tham, J. Varghese, and J. R. Heath, Nat. Nanotechnol. **5**, 718 (2010).
[6]J.-H. Lee, G. A. Galli, and J. C. Grossman, Nano Lett. **8**, 3750 (2008).
[7]Y. Cao, J. He, and J. Sun, Mater. Lett. **63**, 148 (2009).
[8]H. J. Fan, M. Knez, R. Scholz, K. Nielsch, E. Pippel, D. Hesse, M. Zacharias, and U. Gosele, Nature Mater. **5**, 627 (2006).
[9]R. Srinivasan, M. Jayachandran, and K. Ramachandran, Cryst. Res. Technol. **42**, 266 (2007).
[10]L. C. L. Y. Voon, Y. Zhang, B. Lassen, M. Willatzen, Q. Xiong, and P. C. Eklund, J. Nanosci. Nanotechnol. **8**, 1 (2008).
[11]Z. Sui and I. P. Herman, Phys. Rev. B **48**, 17938 (1993).
[12]A. Paul, M. Luisier, and G. Klimeck, J. Comput. Electron. **9**(3), 160 (2010).
[13]A. Paul, M. Luisier, and G. Klimeck, 14th International Workshop on Computational Electronics (IWCE), 26–29 October 2010, Pisa, pp. 1–4.
[14]R. Landauer, IBM J. Res. Dev. **1**, 223 (1957).
[15]T. Markussen, A.-P. Jauho, and M. Brandbyge, Nano Lett. **8**, 3771 (2008).
[16]N. Mingo, L. Yang, D. Li, and A. Majumdar, Nano Lett. **3**, 1713 (2003).
[17]H. Peelaers, B. Partoens, and F. M. Peeters, Nano Lett. **9**, 107 (2009).
[18]A. Palaria, G. Klimeck, and A. Strachan, Phys. Rev. B **78**, 205315 (2008).
[19]J. Chen, G. Zhang, and B. Li, Nano Lett. **10**, 3978 (2010).
[20]A. Bodapati, P. K. Schelling, S. R. Phillpot, and P. Keblinski, Phys. Rev. B **74**, 245207 (2006).